

# Research Assistantship Progress Report

Supervisor: Dr. Maria Cameron

Abdullah Ahmed

Department of Mathematics at University of Maryland, College Park,  
Spring 2025

This document is structured chapter-wise according to different papers read.

## Contents

<b>1</b>	<b>Asymptotic Analysis of Bifurcations in Feedforward Networks. [1]</b>	<b>2</b>
1.1	Introduction . . . . .	2
1.2	Background . . . . .	2
1.3	Steady-State Bifurcation with two cells . . . . .	3
1.4	Diversion . . . . .	4
1.5	Steady-State Bifurcation with three cells . . . . .	5
1.6	Hopf Bifurcation with 3 cells and $\gamma = 0$ . . . . .	6
1.7	Hopf Bifurcation with 3 cells and $\gamma \neq 0$ . . . . .	8
1.8	Extension to non-homogeneous case . . . . .	9
1.8.1	Steady-State Bifurcation with non-homogeneity (Qualitative study)	9
1.8.2	Steady-State Bifurcation with non-homogeneity (Quantitative study)	11
1.8.3	Hopf Bifurcation with non-homogeneity in $\omega$ . . . . .	14
1.8.4	Hopf Bifurcation with non-homogeneity in $\mu$ . . . . .	15
1.9	Discussion . . . . .	16

# 1 Asymptotic Analysis of Bifurcations in Feedforward Networks. [1]

## 1.1 Introduction

The *normal* form of the Hopf bifurcation is given by  $\dot{z} = (\mu + i\omega)z - (1 + i\gamma)|z|^2z$ . After the bifurcation point  $\mu = 0$ , there is a stable limit cycle at  $r = \sqrt{\mu}$  when  $\mu > 0$ . This can be seen by converting the equation into polar form using  $z(t) = r(t)e^{i\theta(t)}$  which gives the system:

$$\begin{aligned}\dot{r}(t) &= \mu r - r^3 \\ \dot{\theta} &= \omega - \gamma r^2.\end{aligned}\tag{1}$$

As one can note, the amplitude of this oscillation increases at a relatively slow rate around the bifurcation point.

With coupled systems, as we shall see, it is possible to achieve a growth rate proportional to  $\mu^{1/6}$  close to the bifurcation point for the amplitude of the subsequent oscillations. It is also possible to achieve a similar rate for pitchfork bifurcations with respect to their equilibria. This gives a much faster growth rate around the bifurcation for small perturbations to  $\mu$ , but one which asymptotically settles onto the usual rate being proportional  $\mu^{1/2}$  for large  $\mu$ .

## 1.2 Background

The coupling of a feed forward network of three cells (each representing a dynamical system undergoing Hopf bifurcation at  $\mu = 0$ ) is governed by introducing another parameter  $\lambda$  (called the *coupling strength*) as follows:

$$\begin{aligned}\dot{z}_1 &= (\mu + i\omega)z_1 - (1 + i\gamma)|z_1|^2z_1 - \lambda z_1 \\ \dot{z}_2 &= (\mu + i\omega)z_2 - (1 + i\gamma)|z_2|^2z_2 - \lambda z_1 \\ \dot{z}_3 &= (\mu + i\omega)z_3 - (1 + i\gamma)|z_3|^2z_3 - \lambda z_2.\end{aligned}\tag{2}$$

This indicates that the first cell is coupled to itself, the second to the first, and the third to the second. As results will show, the Hopf bifurcation in the third cell displays the faster growth rate mentioned before. In fact, the stronger fact is true that with  $n$  coupled cells, the growth rate is proportional to  $\mu^{1/2(3)^{n-2}}$ .

### 1.3 Steady-State Bifurcation with two cells

We first look at instances of this peculiar growth rate in pitchfork bifurcations. Consider the simple 2-cell coupled system with the only the second cell coupled to the first:



$$\begin{aligned}\dot{x} &= \mu x - x^3, \\ \dot{y} &= \mu y - y^3 - \lambda x.\end{aligned}$$

As the first cell is uncoupled, it simply represents the usual supercritical pitchfork bifurcation, with the bifurcation value being  $\mu_c = 0$ , and fixed points occurring at  $x = 0, \pm\sqrt{\mu}$ . Corresponding to  $x = 0$ , the second cell displays fixed points at  $y = 0, \pm\sqrt{\mu}$ . This is simple enough, as this behavior of the second cell is also the typical supercritical pitchfork bifurcation. It is the corresponding uncoupled behavior of the second cell for  $x = \pm\sqrt{\mu}$  that the increased growth rate occurs.

We get two corresponding equations:

$$\dot{y} = f_1(y) = \mu y - y^3 + \lambda\sqrt{\mu} \quad (3)$$

$$\dot{y} = f_2(y) = \mu y - y^3 - \lambda\sqrt{\mu}. \quad (4)$$

Calculating the discriminant of each of the polynomials gives us  $D_1 = D_2 = \frac{-27\lambda^2\mu + 4\mu^3}{108}$ , which is negative for  $0 < \mu < \frac{3\sqrt{3}\lambda}{2}$ , and hence only one real root for these values of  $\mu$ .

Note that by Descartes' Rule of Signs, as  $\mu, \lambda > 0$ ,  $f_1$  has a positive root, while  $f_2$  has a negative root, due to there being only one sign change in  $f_1(y)$  and  $f_2(-y)$ .

Considering  $f_1$  and  $f_2$  as now functions of two variables with additional dependence on  $\mu$ , we can use the implicit function theorem now allows us to get a unique local representation of how the fixed points in the second cell (given by  $f_i(\mu, y) = 0$ ) vary with small perturbations  $\mu$ , i.e, give us a nice function  $y = \phi_i(\mu)$  representing the solution set locally. This is possible as long as  $y^2 \neq \mu/2$  (ensuring  $\frac{\partial f_i}{\partial y} \neq 0$ ), which is satisfied for  $\mu \in (0, 3\sqrt{3}\lambda/2)$ . This is why this is the interval of choice studied above.

Only for  $\mu = 0, 3\sqrt{3}\lambda/2$  is  $y^2 = \mu/2$  a fixed point for the systems above. Moreover as  $f_1(-y) = -\mu y + y^3 + \lambda\sqrt{\mu} = -f_2(y)$ , uniqueness in the implicit function theorem implies  $\phi_1 = -\phi_2$ . Thus we shall refer to them as simply  $\pm\phi$  respectively.

It is also possible to see that for  $\mu \in (0, 3\sqrt{3}\lambda/2)$ ,  $|\phi(\mu)|^2 > \mu/3$ , by examining existence of positive roots for  $f_i(y + \sqrt{\mu/3})$ . And thus, given the fixed points in the second cell by  $\phi(\mu)$ , with the inequality above, we may characterize the nature of these fixed

points by looking at the linearization of the system through its Jacobian:

$$\mathbf{J} = \begin{pmatrix} \mu - 3x^2 & 0 \\ -\lambda & \mu - 3y^2 \end{pmatrix}$$

Looking at the eigenvalues on the diagonal and evaluating at the fixed points gives us the following classification:  $(0, 0)$  is a source,  $(0, \pm\sqrt{\mu})$  are saddle points (unstable in the  $x$ -direction), and  $\pm(\sqrt{\mu}, \phi(\mu))$  are stable fixed points (in fact, a stable *branch* of fixed points) for  $\mu \in (0, 3\sqrt{3}\lambda/2)$ .

Finally, we can now qualify the behaviour of  $\phi(\mu)$  for  $\mu$  close to 0. Note that as  $\mu$  goes to 0, the behaviour of  $f_1(y)$  is dominated by the  $-y^3$  term, and so the roots of  $f_1$  approach 0, that is,  $\phi(\mu)$  goes to 0 as well. Thus we have:

$$\begin{aligned} f_1(\phi(\mu)) &= \mu\phi(\mu) - \phi(\mu)^3 + \lambda\sqrt{\mu} = 0 \\ \frac{\phi(\mu)^3}{\lambda\sqrt{\mu}} &= 1 + \sqrt{\mu}\phi(\mu). \end{aligned}$$

Thus taking the limit as  $\mu \rightarrow 0$ , we have  $\phi(\mu)^3 \sim \lambda\sqrt{\mu}$ . Thus  $\phi(\mu) \sim \lambda^{1/3}\mu^{1/6}$  for small  $\mu$ .

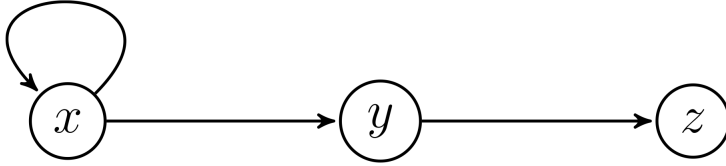
## 1.4 Diversion

The network above, although useful in its simplicity for depicting the atypical growth rate, lacks many characteristics that may be desirable in a network geared for practical applications. One such characteristic is of the presence of *synchrony*, a phenomenon where certain cells depict identical dynamics due to some form of symmetry present in the network. As it turns out, perfect symmetry is not needed for this phenomenon to occur, and indeed this more generalized notion is more realistic and robust in displaying synchrony.

This generalized notion is that of the existence of a *balanced coloring*, which is a coloring that respects some equivalence relation on cells and the edges corresponding to the *inputs* of any cell. This implies the existence of *robust patterns of synchrony* for *admissible* ODEs (that respect the coloring). The robustness implies that they persist through small perturbations to the underlying ODEs (a characteristic not displayed with perfect symmetry). Moreover, the *quotient* graphs formed by identifying equivalent edges and cells, allows the study of the ODEs to be restricted to these *clusters* of synchronuous nodes, which often displays simplified dynamics. As it turns out, the simplest such network is our next example.

## 1.5 Steady-State Bifurcation with three cells

Now assume we work in a slightly more complicated setting with three cells with coupling:



$$\begin{aligned}\dot{x} &= \mu x - x^3 - \lambda x, \\ \dot{y} &= \mu y - y^3 - \lambda x, \\ \dot{z} &= \mu z - z^3 - \lambda y.\end{aligned}$$

First we note that the first cell does not undergo a bifurcation until  $\mu = \lambda$ , and so for  $\mu < \lambda$ , the first cell only has its trivial fixed point at  $x = 0$ . But at this fixed point value, the second cell becomes decoupled from the first, and cells 2 and 3 act as an independent 2-cell system identical to the one above. And so for  $0 < \mu < \lambda < \frac{3\sqrt{3}\lambda}{2}$ , the same argument applies and gives us the same fixed points as before in the third cell being given by  $\pm\phi(\mu)$ . To characterize the stability of these fixed points, we compute the Jacobian:

$$\mathbf{J} = \begin{pmatrix} \mu - \lambda - 3x^2 & 0 & 0 \\ -\lambda & \mu - 3y^2 & 0 \\ 0 & -\lambda & \mu - 3z^2 \end{pmatrix}$$

with clearly negative eigenvalues for  $x = 0$ ,  $y = \pm\sqrt{\mu}$ ,  $z = \pm\phi(\mu)$ . Hence, these fixed points are stable. Moreover, the fixed points of cell 3 inherit the same  $\mu^{1/6}$  growth in their amplitude.

That said, what happens for large  $\mu$ ? For large  $\mu > \lambda$ , consider the fixed point at  $x = \sqrt{\mu - \lambda}$ , and plug this into the second cell's dynamics to note that the corresponding fixed points are given by:

$$y = \frac{y^3}{\mu} + \lambda \frac{\sqrt{\mu - \lambda}}{\mu}. \quad (5)$$

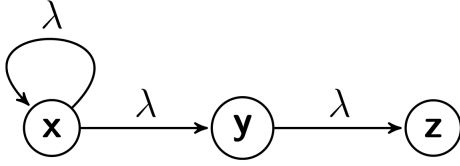
And so,  $y \rightarrow 0$  as  $\mu \rightarrow \infty$ . As the corresponding fixed points of the second cell coalesce at 0, the corresponding fixed points in cell 3 are given by:

$$\mu z = z^3.$$

Hence we recover the  $z \sim \mu^{1/3}$  growth. Thus, our exotic phenomenon is short-lived.

## 1.6 Hopf Bifurcation with 3 cells and $\gamma = 0$

Our model is given by:



$$\begin{aligned}\dot{x} &= (\mu + i\omega)x - (1 + i\gamma)|x|^2x - \lambda x, \\ \dot{y} &= (\mu + i\omega)y - (1 + i\gamma)|y|^2y - \lambda x, \\ \dot{z} &= (\mu + i\omega)z - (1 + i\gamma)|z|^2z - \lambda y.\end{aligned}$$

with  $\gamma = 0$ .

We now proceed with a standard technique used to approximate analytic solutions to systems of ODES. First we consider a perturbative approach by suppressing nonlinearities by multiplying by a scale term  $\epsilon$  to get:

$$\begin{aligned}\dot{x} &= (\epsilon\mu + i\omega)x - \epsilon|x|^2x - \epsilon\lambda x \\ \dot{y} &= (\epsilon\mu + i\omega)y - \epsilon|y|^2y - \epsilon\lambda x \\ \dot{z} &= (\epsilon\mu + i\omega)z - \epsilon|z|^2z - \epsilon\lambda y.\end{aligned}\tag{6}$$

Now we have two time scales to deal with in the problem, one on the order of  $\epsilon^{-1}$  and one on the order of  $\omega^{-1}$ . The rough idea of the technique is to assume the time scales are different enough so that the dynamics can be considered as independent functions of the two times  $\eta = \epsilon t$  and  $\xi = \omega t$ . We now assume we can do a Taylor expansion in these variables:

$$\begin{aligned}x(\xi, \eta) &= x_0(\xi, \eta) + \epsilon x_1(\xi, \eta) + \epsilon^2 x_2(\xi, \eta) + \dots \\ y(\xi, \eta) &= y_0(\xi, \eta) + \epsilon y_1(\xi, \eta) + \epsilon^2 y_2(\xi, \eta) + \dots \\ z(\xi, \eta) &= z_0(\xi, \eta) + \epsilon z_1(\xi, \eta) + \epsilon^2 z_{,2}(\xi, \eta) + \dots\end{aligned}\tag{7}$$

Noting that  $d/dt = \omega d/d\xi + \epsilon d/d\eta$  by the chain rule, we may plug in our approximation into (7), and separate powers of  $\epsilon$ . As the equations must hold for all  $\epsilon$  sufficiently small enough, we may equate coefficients of powers of  $\epsilon$ . The terms upto order  $\epsilon$  are:

$$\begin{aligned}(\text{R.H.S}) &= \frac{dx}{dt} = \omega \frac{\partial x}{\partial \xi} + \epsilon \frac{\partial x}{\partial \eta} \\ &\approx \omega \frac{\partial x_0}{\partial \xi} + \epsilon \frac{\partial x_0}{\partial \eta} + \epsilon \left( \omega \frac{\partial x_1}{\partial \xi} \right) \\ &= \epsilon \left( \frac{\partial x_0}{\partial \eta} + \omega \frac{\partial x_1}{\partial \xi} \right) + \omega \frac{\partial x_0}{\partial \xi} \\ &= (\text{L.H.S}) = \epsilon(\mu x_0 + i\omega x_1 - |x_0|^2 x_0 - \lambda x_0) + (i\omega x_0).\end{aligned}$$

and similarly for  $y$  and  $z$ . This yields overall:

$$\begin{aligned}\frac{\partial x_0}{\partial \xi} &= ix_0 \\ \frac{\partial y_0}{\partial \xi} &= iy_0 \\ \frac{\partial z_0}{\partial \xi} &= iz_0\end{aligned}\tag{8}$$

$$\begin{aligned}\omega \frac{\partial x_1}{\partial \xi} &= i\omega x_1 - \frac{\partial x_0}{\partial \eta} + \mu x_0 - |x_0|^2 x_0 - \lambda x_0 \\ \omega \frac{\partial y_1}{\partial \xi} &= i\omega y_1 - \frac{\partial y_0}{\partial \eta} + \mu y_0 - |y_0|^2 y_0 - \lambda y_0 \\ \omega \frac{\partial z_1}{\partial \xi} &= i\omega z_1 - \frac{\partial z_0}{\partial \eta} + \mu z_0 - |z_0|^2 z_0 - \lambda z_0.\end{aligned}\tag{9}$$

The system (8) has solutions of the form  $x_0(\xi, \eta) = A(\eta)e^{i\phi_1(\eta)}e^{i\xi}$ , and we may plug this into the system given in (9) to get:

$$\omega \frac{\partial x_1}{\partial \xi} = i\omega x_1 - ((A'(\eta) + i\phi_1'(\eta) - \mu + A(\eta)^2 + \lambda)A(\eta))e^{i\phi_1(\eta)}e^{i\xi}.\tag{10}$$

Note that the second term is a resonant forcing term, and will cause the solution to blow up as  $\xi \rightarrow \infty$ . Such terms in the solution are called **secular**, and are set to 0 in two-time scale calculations. These yield the following equations for the three cells:

$$\begin{aligned}A' + iA\phi' &= \mu A - A^3 - \lambda A \\ B' + iB\phi' &= \mu B - B^3 - \lambda A e^{i(\phi_1 - \phi_2)} \\ C' + iC\phi' &= \mu C - C^3 - \lambda B e^{i(\phi_2 - \phi_3)},\end{aligned}\tag{11}$$

where A,B,C are approximations to the amplitude of oscillations in cell 1, 2, and 3 respectively, and  $\phi_i$  represent the phase of each corresponding cell. Seperating into real and imaginary parts, and setting  $\psi_1 = \phi_1 - \phi_2$  and  $\psi_2 = \phi_2 - \phi_3$ :

$$\begin{aligned}A' &= \mu A - A^3 - \lambda A \\ B' &= \mu B - B^3 - \lambda A \cos(\psi_1) \\ C' &= \mu C - C^3 - \lambda B \cos(\psi_2) \\ \psi_1' &= (\lambda A/B) \sin(\psi_1) \\ \psi_2' &= (\lambda B/C) \sin(\psi_2) - (\lambda A/B) \sin(\psi_1).\end{aligned}\tag{12}$$

We can note that  $\psi_i$  have fixed points for  $\psi_i = n\pi$ ,  $n \in \mathbb{Z}$  (denoting limit cycles), and so the first three equations become:

$$\begin{aligned} A' &= \mu A - A^3 - \lambda A \\ B' &= \mu B - B^3 \pm \lambda A \\ C' &= \mu C - C^3 \pm \lambda B. \end{aligned} \tag{13}$$

The stability of this system can be analyzed as before for  $0 < \mu < \lambda$  to obtain similar results, and we may also note the same  $\sim \mu^{1/6}$  growth rate in cell 3. Finally, we may solve the 1st-order equations in (9) to obtain full solutions approximate to order  $\epsilon$ . Note that these will still only give a qualitative picture for the original system with  $\epsilon = 1$  (and hence for  $t \sim 1$ ). For greater  $t$ , we cannot ignore higher order terms, but the picture suffices us for gaining insight into the bifurcation behavior.

## 1.7 Hopf Bifurcation with 3 cells and $\gamma \neq 0$

Similar two-time scale analysis will lead us to the following slightly more complicated system:

$$\begin{aligned} A' &= \mu A - A^3 - \lambda A \\ B' &= \mu B - B^3 - \lambda A \cos(\psi_1) \\ C' &= \mu C - C^3 - \lambda B \cos(\psi_2) \\ \psi_1' &= \gamma(B^2 - A^2) + (\lambda A/B) \sin(\psi_1) \\ \psi_2' &= \gamma(C^2 - B^2) + (\lambda B/C) \sin(\psi_2) - (\lambda A/B) \sin(\psi_1). \end{aligned} \tag{14}$$

To deal with the simpler case first, we consider  $A = 0$ , which decouples  $\psi_1$  from the system. Then we do some algebraic manipulations in the third and fifth equations as we solve for the equilibrium:

$$C^2(\mu - C^2)^2 = \lambda^2 B^2 \cos^2(\psi_2), \quad \gamma^2 C^2(C^2 - B^2) = \lambda^2 B^2 \sin^2(\psi_2),$$

to finally get:

$$\begin{aligned} 0 &= \mu B - B^3 \\ \lambda^2 B^2 &= C^2(\mu - C^2)^2 + \gamma^2 C^2(C^2 - B^2). \end{aligned} \tag{15}$$

For  $B = \pm\sqrt{\mu}$ , the second equation simplifies to a familiar form:

$$\mu C - C^3 \pm \lambda \sqrt{\frac{\mu}{1 + \gamma^2}},$$



and the rest of the analysis follows as usual, (one can check that  $C$  decreases with  $\gamma$ ).

For  $A = \pm\sqrt{\mu - \bar{\lambda}}$ , we cannot ignore  $\psi_1$ . We assume that there exists a solution for  $\psi_1$  such that  $\psi'_1 = 0$ , and substitute the relation  $\sin(\psi_1) = \frac{\gamma B(A^2 - B^2)}{\lambda A}$  from the third equation in (14) to get:

$$\begin{aligned} 0 &= (\mu - \lambda)A - A^3 \\ \lambda^2 A^2 &= B^2(\mu - B^2)^2 - \gamma^2 B^2(B^2 - A^2)^2 \\ \lambda^2 B^2 &= C^2(\mu - C^2)^2 - \gamma^2 C^2(C^2 - A^2)^2, \end{aligned} \tag{16}$$

which has a synchronous solution  $A, B, C = \pm\sqrt{\mu - \bar{\lambda}}$ . But if  $|\frac{\gamma B(A^2 - B^2)}{\lambda A}| > 1$ ,  $\psi'_1 \neq 0$ , and the system does not settle into equilibrium, and displays quasi-periodic behavior.

## 1.8 Extension to non-homogeneous case

So far we have assumed that most physical parameters that define different cells are exactly the same, but this may not be the case in practice due to manufacturing errors. Moreover, it is interesting in it's own right to extend our study to understand the effect of non-homogeneity on the bifurcation behavior.

### 1.8.1 Steady-State Bifurcation with non-homogeneity (Qualitative study)

Assume our two-cell system is given as:

$$\begin{array}{c} \boxed{x} \longrightarrow \bigcirc y \end{array} \quad \begin{aligned} \dot{x} &= \mu x - x^3 \\ \dot{y} &= (\mu + \epsilon)y - y^3 - \lambda x. \end{aligned}$$

where  $\epsilon$  is a constant.

Note firstly that the dynamics of the first cell are unchanged, and we have fixed points occurring at  $x = 0$  only for  $\mu < 0$ , and additionally  $x = \pm\sqrt{\mu}$  for  $\mu > 0$ . For  $x = 0$ , the corresponding fixed points in the second cell are also given simply by  $y = 0, \pm\sqrt{\mu + \epsilon}$  depending on whether  $\mu + \epsilon > 0$ . Looking at the Jacobian:

$$\mathbf{J} = \begin{pmatrix} \mu - 3x^2 & 0 \\ -\lambda & \mu + \epsilon - 3y^2 \end{pmatrix}$$

we can easily categorize the stability of these fixed points by evaluating the eigenvalues  $\mu - 3x^2$  and  $\mu + \epsilon - 3y^2$ .

$x$	$y$	$\lambda_1$	$\lambda_2$
0	0	$\mu$	$\mu + \epsilon$
0	$\sqrt{\mu + \epsilon}$	$\mu$	$2\mu + 2\epsilon$
0	$-\sqrt{\mu + \epsilon}$	$\mu$	$2\mu + 2\epsilon$

Let us consider the more interesting case corresponding to  $x = \pm\sqrt{\mu}$ . That is, we look at the roots of the polynomials  $y^3 - (\mu + \epsilon)y \pm \lambda\sqrt{\mu}$ .

The discriminant of the depressed cubics above is given by:

$$D = -4(-(\mu + \epsilon))^3 - 27(\pm\lambda\sqrt{\mu})^2 = 4(\mu + \epsilon)^3 - 27\lambda^2\mu. \quad (17)$$

Let  $f(\mu) = D$ .

Note now that the case for  $\epsilon < 0$  is qualitatively similar to  $\epsilon = 0$ , that is, there is one fixed point until some positive value of  $\mu$ , after which there are three. This can be argued as follows: for  $\epsilon < 0$ , we can see for that for  $0 < \mu < |\epsilon|$ ,  $f(\mu) < 0$ , and moreover, the coefficient of the cubic term in  $f$  is positive, that is,  $f \rightarrow \infty$  as  $\mu \rightarrow \infty$ . Expanding  $f$  we get:

$$f(\mu) = 4\mu^3 + 12\mu^2\epsilon + (12\epsilon^2 - 27\lambda^2)\mu + 4\epsilon^3.$$

For  $\epsilon < 0$ , by the Descartes Rule of Signs,  $f$  has either 1 or 3 positive roots, contingent on whether  $(12\epsilon^2 - 27\lambda^2) < 0$ , which is equivalent to  $\epsilon < 1.5\lambda$ . We may rule out 3 positive roots (occurs only possibly when  $\epsilon < -1.5\lambda$ ) as follows: first note that the derivative  $f'(\mu) = 12(\mu + \epsilon)^2 - 27\lambda^2$  has two roots at  $\mu = \pm 1.5\lambda - \epsilon$ , which are both positive. For there to be 3 roots, the corresponding stationary value for the smaller root:

$$f(-1.5\lambda - \epsilon) = 27\lambda^3 + 27\lambda^2\epsilon,$$

should be positive, but it is not. Thus as  $f$  has only one root, this implies exactly the same behavior as for  $\epsilon = 0$ . For  $\mu < |\epsilon|$ , the unique fixed point is also guaranteed to be stable.

For  $\epsilon > 0$ , we have indeed a special case. For  $\mu$  small enough,  $D > 0$ . Thus we have 3 fixed points in some neighborhood of  $\mu = 0$  by continuity. Considering the roots of  $f'$  again:  $\mu = \pm 1.5\lambda - \epsilon$ , we can see that for  $\epsilon > 1.5\lambda$ , there are no positive stationary points for  $f$  and  $f'(0) > 0$ , and thus by smoothness, this implies that there are 3 fixed points for all  $\mu > 0$ . For  $\epsilon < 1.5\lambda$ , we do have a stationary point at some positive  $\mu = 1.5\lambda - \epsilon$ . Note that the leading coefficient of the derivative quadratic is positive, and this is the bigger root, and so  $f' > 0$  for  $\mu > 1.5\lambda - \epsilon$ . This gives two cases: either there are always 3 fixed points, or 2 of the fixed points coalesce and annihilate and leave 1 fixed point, until eventually there are 3 fixed points again. This

can be characterized by whether the stationary value of  $f$  is positive or negative:

$$f(1.5\lambda - \epsilon) = -27\lambda^3 + 27\lambda^2\epsilon.$$

Thus for  $\epsilon < \lambda$ , the value is negative, and we have the transition from three to one to three fixed points, and for  $\epsilon > \lambda$  we always have 3 fixed points.

### 1.8.2 Steady-State Bifurcation with non-homogeneity (Quantitative study)

Now to quantify the growth rates for this exotic new fixed points, we perform the following analysis for the polynomial:

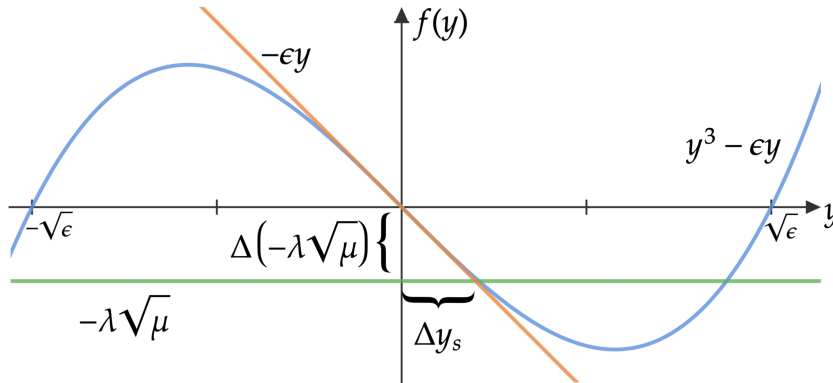
$$y^3 - (\mu + \epsilon)y + \lambda\sqrt{\mu}.$$

First note that by the Descartes Rule of signs, for  $\mu, \epsilon > 0$ , the above polynomial has one negative root, and hence the other two roots for  $\mu$  small enough have to be positive. As the roots continuously depend on the coefficients of the polynomial, and we had one negative root for  $\epsilon = 0$  as well, we can know that the new exotic roots are the positive ones. We study the growth rate of these roots first, noting also that the growth rate for the negative root will also be significantly different from  $\mu^{1/6}$ .

For  $\mu \ll \epsilon$ , we have that the following estimates:

$$\Rightarrow y^3 - \epsilon y \approx -\lambda\sqrt{\mu}. \quad (18)$$

Now we make a geometric argument. The solution to the above equation is given by the intersection of the cubic curve  $y^3 - \epsilon y$  and the horizontal line at  $-\lambda\sqrt{\mu}$ . The cubic curve has roots at  $y = \pm\sqrt{\epsilon}, 0$  and has  $y'(0) = -\epsilon, y'(\pm\sqrt{\epsilon}) = 2\epsilon$ . For  $\mu$  small, we can see that the intersection points will be near these roots by continuity, and in fact will approach these roots as  $\mu \rightarrow 0$ . Thus, we can note that for  $\mu$  small, the change in the intersection value for  $y$  can be approximated up to first order by the derivative at the roots.



For instance, when the smaller positive root  $y_s$  is near 0:

$$\begin{aligned}
\frac{\Delta(y_s)}{\Delta(\mu)} &= \frac{1}{\frac{\Delta(\mu)}{\Delta(y_s)}} \\
&= \frac{-\lambda}{2\sqrt{\mu}} \frac{1}{\frac{\Delta(-\lambda\sqrt{\mu})}{\Delta(y_s)}} \\
&= \frac{-\lambda}{2\sqrt{\mu}} \frac{1}{\frac{\Delta(y_s^3 - \epsilon y_s)}{\Delta(y_s)}} \\
&= \frac{\lambda}{2\epsilon\sqrt{\mu}}.
\end{aligned}$$

This implies that  $y_s \approx \frac{\lambda\sqrt{\mu}}{\epsilon}$  for the smaller positive root. This is similar to what one would get if one were to implicitly differentiate on both sides of (22) with respect to  $\epsilon$  and let  $y$  approach the roots of the approximate cubic. We verify this numerically as well:

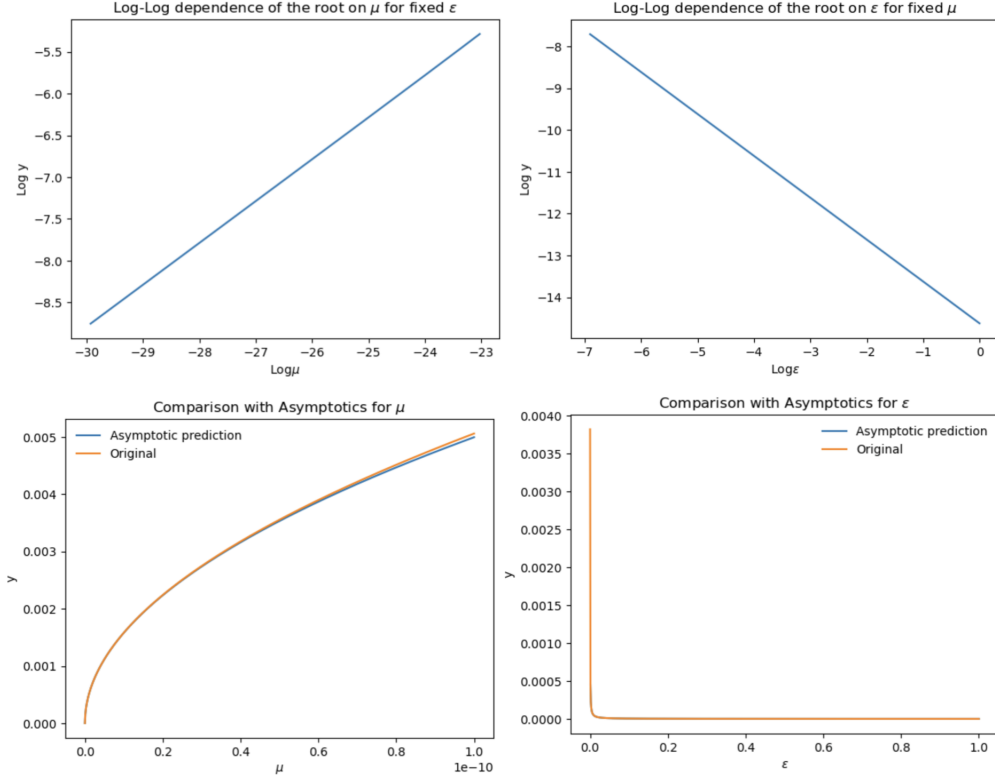


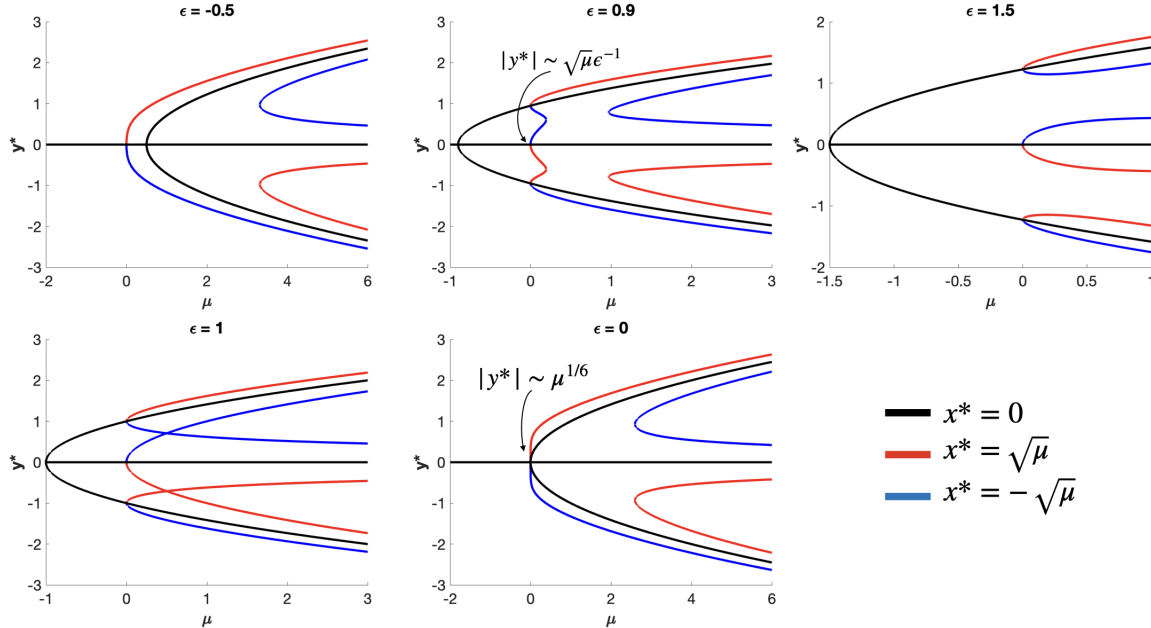
Figure 1: The gradients are respectively 0.5 and -1, and so matches  $y \sim \sqrt{\mu}\epsilon^{-1}$ .

Similarly, for the bigger positive root we have  $y_b \approx \sqrt{\epsilon} - \frac{\lambda\sqrt{\mu}}{2\epsilon}$ , and for the negative root we have  $y_n \approx -\sqrt{\epsilon} - \frac{\lambda\sqrt{\mu}}{2\epsilon}$ .

Note that this growth rate is only effective for  $\mu \ll \epsilon$ , and thus requires enough or more precision in  $\mu$  than  $\epsilon$ . Although this growth rate is slower than  $\mu^{1/6}$  for small values of  $\mu$ , it becomes faster for  $\mu > \epsilon^3$ , and has more sustained growth for larger intervals of  $\mu$ . This also allows us to quantify the nature of the fixed points for small  $\mu$ :  $y_s$  is a saddle point, while  $y_n$  and  $y_b$  are stable fixed points.

**Note:** The growth rate for  $\epsilon < 0$  is similarly  $-\frac{\lambda\sqrt{\mu}}{\epsilon}$ . Also, evaluating the fixed points at  $x = -\sqrt{\mu}$  gives the same growth rates but with opposite sign. And expectedly, in all of these cases, it is easy to see that as  $\mu \rightarrow \infty$ , the  $\epsilon$ -term becomes insignificant, and the growth stabilizes to the usual  $\sim \sqrt{\mu}$ .

Our results can be summarized by the bifurcation diagrams below:



The calculation with 3 cells for the system follows as before:

$$\begin{aligned}
 \dot{x} &= \mu x - x^3 - \lambda_1 x \\
 \dot{y} &= (\mu + \epsilon_1)y - y^3 - \lambda_2 x \\
 \dot{z} &= (\mu + \epsilon_2)z - z^3 - \lambda_3 y.
 \end{aligned} \tag{19}$$

For  $0 < \mu < \lambda_1$ , the first cell has not undergone a bifurcation and hence only has one fixed point at  $x = 0$ . For this fixed point, the second cell and third cell become an

independent system as before with modified parameters:

$$\begin{aligned}\dot{y} &= (\tilde{\mu})y - y^3 \\ \dot{z} &= (\tilde{\mu} + \tilde{\epsilon})z - z^3 - \tilde{\lambda}y,\end{aligned}\tag{20}$$

where  $\tilde{\mu} = \mu + \epsilon_1$ ,  $\tilde{\epsilon} = \epsilon_2 - \epsilon_1$  and  $\tilde{\lambda} = \lambda_3$ . The rest of the analysis follows exactly as above.

### 1.8.3 Hopf Bifurcation with non-homogeneity in $\omega$

Assume our two-cell system is given as:

$$\begin{array}{c} \boxed{x} \longrightarrow \bigcirc y \end{array} \quad \begin{aligned}\dot{x} &= (\mu + i\omega_0)x - |x|^2x, \\ \dot{y} &= (\mu + i\omega)y - |y|^2y - \lambda x.\end{aligned}$$

where  $\omega = \omega_0 + \epsilon\sigma$ , for  $\sigma$  being a detuning parameter.

Standard two-timing calculations give us the system:

$$\begin{aligned}A' &= \mu A - A^3 \\ B' &= \mu B - B^3 - \lambda A \cos(\psi) \\ B\psi' &= -\lambda A \sin(\psi) - \sigma B.\end{aligned}\tag{21}$$

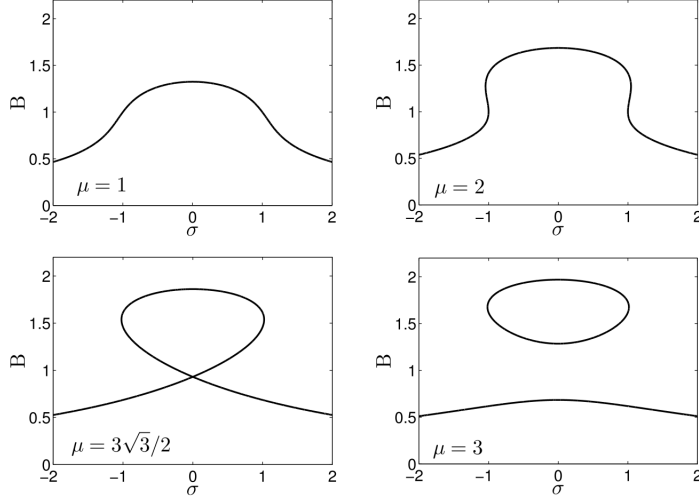
Assuming a fixed point for  $\psi$  exists, the equations reduce to:

$$\begin{aligned}0 &= \mu A - A^3 \\ \lambda^2 A^2 &= \sigma^2 B^2 + B^2(\mu - B^2)^2.\end{aligned}\tag{22}$$

Corresponding to  $A = \pm\sqrt{\mu}$ , we need to solve the following equation for  $B$ :

$$\lambda^2 \mu = \sigma^2 B^2 + B^2(\mu - B^2)^2.\tag{23}$$

We have the following numerical simulations to check our intuition:



Note that in our calculations above, a solution for  $A \neq 0$  only exists if (similar to the sine condition before):

$$|\sigma| \leq \left| \frac{\lambda\sqrt{\mu}}{B^*} \right|, \quad (24)$$

where  $B^*$  are values that satisfy (19). This can be seen to fail above for certain values of  $\sigma$  and  $\mu$  in the last two pictures. Also note, that the emergence of multiple solutions of  $B$  is also similar to our calculations before where we restricted to a certain interval  $0 < \mu < 3\sqrt{3}\lambda/2$ . In particular, this implies we cannot do a quantitative calculation for the dependence of the growth rate on  $\sigma$ , as for  $\mu \rightarrow 0$ ,  $\sigma$  will not be able to satisfy (24), and we will not have a non-trivial equilibrium solution.

#### 1.8.4 Hopf Bifurcation with non-homogeneity in $\mu$

Suppose instead we had the system:

$$\begin{aligned} \dot{x} &= (\mu + i\omega)x - |x|^2x \\ \dot{y} &= ((\mu + \epsilon) + i\omega)y - |y|^2y - \lambda x. \end{aligned} \quad (25)$$

Two-time scale analysis eventually gives us, very similar to above:

$$\lambda^2\mu = ((\mu + \epsilon)^2B^2 - 2(\mu + \epsilon)B^4 + B^6) \quad (26)$$

for non-trivial equilibrium solutions. We know that as  $\mu \rightarrow 0$ ,  $B \rightarrow 0$ . To approximate  $B$  as a function of  $\epsilon$  for  $\mu \ll \epsilon$ , we get the approximation:

$$\lambda^2\mu = \epsilon^2B^2, \quad (27)$$

which gives  $B \sim \lambda\sqrt{\mu}\epsilon^{-1}$ .

## 1.9 Discussion

It can be easily shown that if we consider a more general coupled system of the form:

$$\begin{aligned}
 \dot{x}_0 &= \mu x - x^n \\
 \dot{x}_1 &= \mu x_1 - x_1^n - x_0 \\
 &\vdots \\
 \dot{x}_N &= \mu x_N - x_N^n - x_{N-1},
 \end{aligned} \tag{28}$$

the exotic growth rate near  $\mu = 0$  for cell  $i$  is given by  $|x_i| \sim \mu^{(n^{i-1}-n^i)}$ , implying we may increase the growth rate indefinitely if we have this idealized system.

This now raises questions about the nature of increased growth rate phenomenon. It seems that the root cause is purely the coupling topology of the network, and the degree of the non-linearity in the system, as we observe the same phenomenon in 1-D pitchfork bifurcation systems (and even in discretized versions of it), where there is no periodic forcing or resonance that could help make sense of it. This implores us to explore this phenomenon for other types of bifurcations, coupling topologies, and mixed non-linearities.



## References

- [1] Tyler Levasseur and Antonio Palacios. Asymptotic analysis of bifurcations in feed-forward networks. *International Journal of Bifurcation and Chaos*, 31(02):2150030, Feb 2021.